THE ASTROPHYSICAL JOURNAL, 546:L123–L126, 2001 January 10

INFRARED SPACE OBSERVATORY'S DISCOVERY OF C_4H_2, C_6H_2, AND BENZENE IN CRL 618

JOSÉ CERNICHARO,[1,2] ANA M. HERAS,[3] A. G. G. M. TIELENS,[4] JUAN R. PARDO,[1,5] FABRICE HERPIN,[1]
MICHEL GUÉLIN,[6] AND L. B. F. M. WATERS[7]

Received 2000 September 6; accepted 2000 October 27; published 2001 January 10

ABSTRACT

We report on the detection with the *Infrared Space Observatory* (*ISO*), for the first time in the circumstellar medium, of the polyacetylenic chains C_4H_2 and C_6H_2 and of benzene (C_6H_6) in the direction of the proto–planetary nebula CRL 618. Surprisingly, the abundances of di- and triacetylene are only a factor of 2–4 lower than that of C_2H_2. Benzene is $\simeq$40 times less abundant than acetylene. We suggest that the chemistry in CRL 618 has been strongly modified by the UV photons coming from the hot central star and by the shocks associated with its high-velocity winds. All the infrared bands arise from a region with kinetic temperatures between 200 and 250 K, probably the photodissociation region associated with the dense torus that surrounds the central star. C_4H_2 and C_6H_2 have also been detected in CRL 2688, so it seems that C-rich proto–planetary nebulae are the best organic chemistry factories in space.

Subject headings: circumstellar matter — infrared: general — ISM: molecules — line: profiles — stars: individual (CRL 618, CRL 2688, NGC 7027)

1. INTRODUCTION

The evolution of transition objects between the asymptotic giant branch (AGB) stage and the planetary nebula phase is known to be exceptional, probably the all-decisive moment, where very efficient mass-loss processes determine the basic morphological, kinematical, and chemical layout of planetary nebulae in the process of formation. The global reshaping of the circumstellar envelopes is dictated in a crucial way by the copious mass ejection which occurs toward the end of the AGB phase. Simultaneously with the erosion of the AGB envelope by these high-velocity winds, UV photons from the central star impinge on the neutral envelope, ionizing the gas and driving an interesting photochemistry that may well lead to an efficient buildup of new, large molecules. It is perhaps at these early evolutionary stages of C-rich proto–planetary nebulae, when important amounts of C_2H_2 and CH_4 are still available in the gas phase, that a new series of small hydrocarbons are formed. These species could be the small bricks from which the large C-rich molecules responsible for the emission in the unidentified infrared bands (UIBs) could be created.

CRL 618 is an extreme example of a proto–planetary nebula with a thick molecular envelope (Bujarrabal et al. 1988) surrounding a B0 star and an ultracompact H II region from which UV radiation, by several orders of magnitude larger than that in CRL 2688, impinges on the envelope. The brightening of the H II region in the 1970s (Kwok & Feldman 1981; Martín-Pintado et al. 1993) and the discovery of molecular gas with velocities up to 200 km s^{-1} (Cernicharo et al. 1989) illustrate the rapid evolution of the central star and its influence on the surrounding AGB ejecta. Herpin & Cernicharo (2000) have reported on the detection of H_2O and OH. These O-bearing species, together with H_2CO (Cernicharo et al. 1989), are not present in the envelope of IRC +10216 (Cernicharo, Guélin, & Kahane 2000), the prototype of AGB C-rich circumstellar envelopes.

In this Letter we report on the first detection in space, outside the solar system, of three new molecular species: C_4H_2 (diacetylene), C_6H_2 (triacetylene), and C_6H_6 (benzene) in the direction of CRL 618. C_4H_2 and C_6H_2 have also been found in CRL 2688.

2. OBSERVATIONS

The observations in our study were performed with the short-wavelength spectrometer (SWS; de Graauw et al. 1996) on board the *Infrared Space Observatory* (*ISO*).[8] The spectra of CRL 618, CRL 2688, and NGC 7027 were obtained using the SWS06 observing mode, which was selected to achieve full resolving power (1000–3000, depending on the wavelength), covering the complete wavelength range of the instrument, 2.38–45.2 μm. For comparison and to support the line identifications, we have used other SWS06 observations of the first two sources covering narrower wavelength intervals (CRL 618 in 5.30–7.10 and 19.50–25.07 μm, CRL 2688 in 15.46–16.50 μm). Likewise, SWS01 observations of the three sources have been included in our study. These observations have a resolution lower by factors of 2 in NGC 7027 and 3 in CRL 618 and CRL 2688. The *ISO* observation numbers are 86301602, 35201637, 33800505, 68800562, 33800604, 55800537, 68800561, and 35102563. The data have been analyzed by using the SWS Interactive Analysis (SIA/IA3) package (Salama et al. 1997; Lahuis et al. 1998). In each case the standard processed data file generated by the off-line processing (OLP) has been taken as the basis for the re-

[1] Instituto de Estructura de la Materia, Departamento de Física Molecular, CSIC, Serrano 121, E-28006 Madrid, Spain; cerni@astro.iem.csic.es.
[2] Visiting scientist at the Division of Physics, Mathematics, and Astronomy, California Institute of Technology, MS 320-47, Pasadena, CA 91125; cerni@submm.caltech.edu.
[3] Astrophysics Division, Space Science Department of ESA, ESTEC, P.O. Box 299, 2200 AG Noordwijk, Netherlands.
[4] Kapteyn Astronomical Institute, P.O. Box 800, 9700 AV Groningen, Netherlands.
[5] Division of Physics, Mathematics, and Astronomy, California Institute of Technology, MS 320-47, Pasadena, CA 91125.
[6] IRAM, 300 rue de la Piscine, 38406 St. Martin d'Hères, France.
[7] University of Amsterdam, Astronomical Institute Anton Pannekoek, Kruislaan 403, 1098 SJ Amsterdam, Netherlands.

[8] Based on observations with *ISO*, an ESA project with instruments funded by ESA member states (especially the PI countries: France, Germany, the Netherlands, and the UK) and with the participation of ISAS and NASA.

duction. Dark current subtraction has been carried out interactively. The high flux and resolution of our observations contribute to make the presence of fringes in the OLP-generated spectra a critical problem. Therefore, special attention has been paid to eliminate fringes, both via the interactive application of the relative spectral response function (RSRF) with an SIA routine (for the SWS06 observations) and by applying SIA methods to the RSRF-corrected data (SWS06 and SWS01 observations). After the generation with SIA of the auto analysis result, flat-fielding, sigma-clipping, and rebinnning have been applied. Each detector scans the wavelength range of the band twice: once up and once down in wavelength. The SWS01 and SWS06 observing modes have been designed such that each wavelength range is scanned twice for redundancy. Memory effects in detector bands 2 (4.08–12 μm) and 4 (29–45.2 μm) cause differences in the overall shapes between the up and down scans. We have corrected these differences by flat-fielding the data to the flux level of the down scan, using an order 2 polynomial. In CRL 618, we have obtained good results for detector band 2 data by applying a new memory effect correction method (Kester et al. 2000), which is based on a physical model for Si : Ga detectors (Fouks & Schubert 1995).

To further confirm the spectral features observed in band 3 (12–29 μm), we have used the Astronomical Observing Template band 4 off-band data as an additional and independent source of information (detectors in bands 3 and 4 are made of different materials). Band 4 off-band data cover the same wavelength range as detector band 3, but they are excluded from the standard SWS spectra because of band 4's lower spectral response and higher noise. However, the good quality and high signal-to-noise ratio of the off-band data in our observations allow us to use them with confidence for the comparison.

The final spectrum between 12.7 and 16.4 μm is shown in Figure 1. Other wavelength ranges, together with a detailed comparison of the infrared spectra of the three objects, is done in the accompanying Letter (Cernicharo et al. 2001).

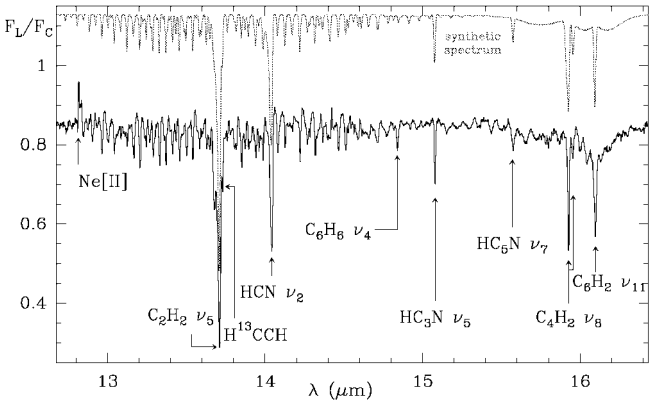

FIG. 1.—Mid-infrared spectrum of CRL 618 around 15 μm. The infrared bands of the polyynes (C_4H_2, C_6H_2), benzene, and cyanopolyynes are indicated by arrows. The thin line corresponds to the synthetic spectrum from the model results discussed in the text for C_2H_2, HCN, C_4H_2, C_6H_2, HC_3N, and HC_5N. The synthetic spectrum for benzene is shown in Fig. 3. All the narrow features to the right and left of the *Q*-branches of C_2H_2 and HCN correspond to the individual rovibrational lines of the *P*- and *R*-branches of these same two species. The individual lines from the bending modes of the other molecular species produce the broad absorption around their *Q*-branches but are not resolved within the spectral resolution of our data. No individual lines of HCN or C_2H_2 are at the frequency of the ν_4 mode of C_6H_6.

3. RESULTS AND DISCUSSION

The wavelength range between 12 and 16.5 μm (see Fig. 1) does show several strong and narrow features of which only those corresponding to HCN and C_2H_2 are also present in IRC +10216 (see Figs. 1 and 2 of Cernicharo et al. 1999). All the other features correspond to the *Q*-branches of the bending modes of heavy species. Two of these features at 15.9 and 16.1 μm arise from the fundamental bending modes ν_8 of C_4H_2 and ν_{11} of C_6H_2. The identification of C_4H_2 and C_6H_2 is further confirmed by the detection of the C_4H_2 combination band $\nu_6 + \nu_8$ at 8 μm and the $\nu_8 + \nu_{11}$ combination band of C_6H_2 at 8.11 μm (see Cernicharo et al. 2001). The laboratory frequencies for these transitions have been taken from Airé & Johns (1992), Haas, Yamada, & Winnewisser (1994a), Haas et al. (1994b), and McNaughton & Bruget (1991, 1992).

In contrast with IRC +10216, where many hot bands of acetylene and HCN have been detected (Cernicharo et al. 1999), CRL 618 shows only the fundamental bands of these molecules. This fact means that the kinetic temperature of the gas is much lower in this source than in IRC +10216.

Using the data for C_2H_2 and HCN described in Cernicharo et al. (1999), we derive a temperature of 200 K for C_2H_2 and HCN and column densities of 2×10^{17} and 1.5×10^{17} cm^{-2}, respectively. For the isotope $H^{13}CCH$, which is clearly detected in Figure 1, we derive $N(H^{13}CCH) = 1.1 \times 10^{16}$ cm^{-2}. Hence, $X(C_2H_2)/X(H^{13}CCH) = 18$ and $X(^{12}C)/X(^{13}C) = 36$. This result is in good agreement with the value derived by Kahane et al. (1992). An upper limit of 250 K for the kinetic temperature of the absorbing gas can be derived from the limits to the intensity of the hot bands of HCN and C_2H_2 in Figure 1. A kinetic temperature of 300 K will produce detectable absorption in the hot bands of these species. In our models we have assumed that the line width of each individual rovibrational transition of HCN and C_2H_2 is 10 km^{-1} (see Cernicharo et al. 2001). The individual lines of the *P*- and *R*-branches of HCN and C_2H_2 are clearly seen in the spectra of Figure 1 and agree in intensity and position with the results of our model.

We have modeled the infrared bending bands of C_4H_2 and C_6H_2 from the laboratory data quoted above. Figure 1 shows the excellent agreement between our data and the models. The kinetic temperature is a key parameter in modeling the absorption of the infrared active modes ν_8 of C_4H_2 and ν_{11} of C_6H_2. Obviously, the shape of the absorption produced by these molecules at around 16 μm will depend on the population of their lowest bending energy levels that will determine the intensity of the associated hot bands. The lowest energy vibrational mode of C_4H_2, ν_9, is at 220 cm^{-1} (317 K) above the ground (Airé & Johns 1992), and the ν_{13} bending mode of C_6H_2 is only at 105 cm^{-1} (151 K) above the ground (Haas et al. 1994c). These levels are so low in energy that they will be significantly populated even at relatively low temperatures. Haas et al. (1994a) present in their Figure 2 a laboratory spectrum at room temperature showing several *Q*-branches of the $\nu_{11} + \nu_{13}$ and $\nu_{11} + 2\nu_{13}$ infrared transitions. These *Q*-branches are as strong as the fundamental one. In modeling our data, we have considered the ν_8 and $\nu_8 + \nu_9$ bands of C_4H_2 but only the fundamental ν_{11} bending mode of C_6H_2, as the individual *Q*-branches of the different hot bands and that of the ν_{11} are unresolved in the *ISO*/SWS data. However, the presence of the hot bands has been taken into account in calculating the column density that fits the intensity of the observed narrow absorption feature. We have adopted the vibrational band strengths given by Khilifi et al. (1995). The best model fitting is obtained for $N(C_4H_2) = 1.2 \times 10^{17}$ cm^{-2} and $N(C_6H_2) = 6 \times 10^{16}$ cm^{-2}. Hence, the abundance of C_6H_2 is

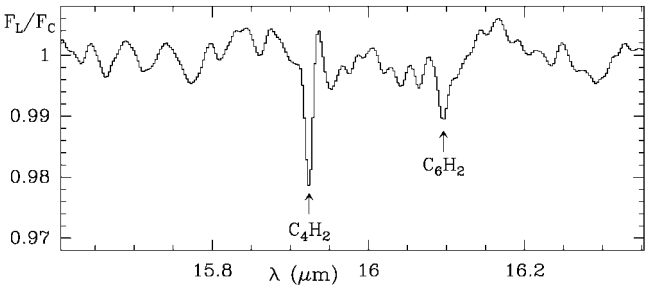

FIG. 2.—*ISO*/SWS spectrum of CRL 2688 around the bending modes of di- and triacetylene.

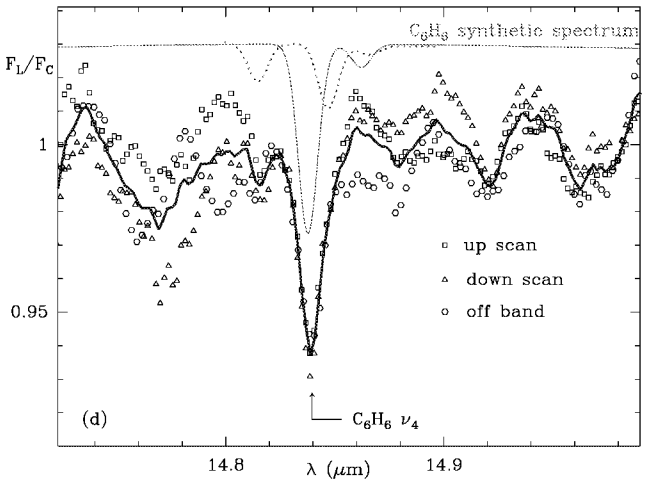

FIG. 3.—*ISO*/SWS spectrum of CRL 618 around the ν_4 bending mode of benzene. The individual markers correspond to up, down, and off-band data as described in the text. The off-band data correspond to a different detector band and are shown here to stress that the feature we identify with the ν_4 mode of benzene is real. The averaged spectrum from these data is plotted as a thick line. The modeled spectrum for benzene is shown by the thin line. The dashed line corresponds to the synthetic spectrum discussed in the text for HCN, the polyynes, and the cyanopolyynes and shown in Fig. 1 (only the wavelength range 14.8–14.89 μm is shown here). The $P(13)$ line of the ν_2 bending mode of HCN contributes with an absorption of 1% in the red wing of C_6H_6.

only a factor of 2 lower than that of C_4H_2, which in turn is also only a factor of 2 below that of C_2H_2. These large abundances are rather surprising and unpredicted by any chemical model so far. The model results in Figure 1 reproduce very well the shape of the absorption for C_4H_2 and its hot band. For C_6H_2, the modeled Q-branch agrees very well with the observations, but around it there is an absorption excess in the data that certainly corresponds to the contribution of the P- and R-branches of the hot bands. In addition, we note that this wavelength range will also be affected by the absorption of CH_3CCH (see Cernicharo et al. 2001). Di- and triacetylene have also been found in the direction of CRL 2688 (see Fig. 2). Besides these species, three other features are prominent in the spectrum of Figure 1. Two of them can be easily identified as the ν_5 and ν_7 bending modes of HC_3N (Yamada & Bürger 1986) and HC_5N (Haas et al. 1994a). These are the strongest infrared bands of these cyanopolyynes. These bands, although strong, are less prominent than those of C_4H_2 and C_6H_2. For $T_K = 200$ K, and using the vibrational band strengths given by Deguchi & Uyemura (1984) for HC_5N and by Uyemura et al. (1982) for HC_3N, we obtained $N(HC_3N) = 5 \times 10^{16}$ cm^{-2} and $N(HC_5N) = 1.5 \times 10^{16}$ cm^{-2}. The last feature in Figure 1, which is as strong as the ν_7 Q-branch of HC_5N, corresponds to benzene.

Figures 1 and 3 show that a narrow feature is centered within a few tenths of the spectral resolution, which is 0.01 μm at this wavelength, of the expected Q-branch of the ν_4 band of benzene (673.9732 cm^{-1}, i.e., 14.8374 μm; Lindemayer, Magg, & Jones 1988). This narrow feature cannot be associated with any of the lines of the P-branch of C_2H_2 and HCN bending modes (see Fig. 1). The $P(13)$ line of HCN at 14.847 μm could contribute with a maximum of 1% of absorption in the red wing of the ν_4 feature (see Fig. 3). In addition, the feature we attribute to benzene is not only visible in each up and down scan individually but also in the off-band data obtained by detector band 4 of the SWS. This provides an independent confirmation of the absorption. C_6H_6 has 20 vibrational modes (Herzberg 1964) of which only four are infrared-active. The bending mode ν_4 (all hydrogens moving away in the same direction from the plane formed by the six carbons) is the strongest infrared band of benzene. Benzene is an oblate symmetric top with a very large density of rotational states. The rotational partition function of its ground state at 200 K is 2.65×10^5 (Dang-Nhu & Plíva 1989); hence, large column densities are needed to produce significant absorption. Fortunately, all the lines in the ν_4 Q-branch are overlapped, producing a relatively strong narrow feature. In contrast, the individual P and R rotational lines, which would be roughly separated at the spectral resolution of the *ISO*/SWS, will produce very weak absorption. A vibrational band strength of 218.5 cm^{-2} atm^{-1} has been measured at 296 K (Dang-Nhu, Blanquet, & Raulin 1988), corresponding to an Einstein coefficient of 5.7 s^{-1}. In addition to the ν_4 transition, we have included in our calculations the hot band $\nu_4 + \nu_{20} \leftarrow \nu_{20}$ at 14.862 μm, where ν_{20} is the lowest frequency vibrational mode of benzene at 398 cm^{-1}. We have assumed that the vibrational band strength for the hot band is similar to that of the fundamental ν_4 (see Kauppinen, Jensen, & Brodersen 1980). The ν_{20} mode is inactive in the infrared. At 300 K 54% of the benzene molecules will be in the ground state while 16% will be in the ν_{20}. At 200 K these numbers change to 85% and 9.5%, i.e., the contribution of the hot band could be hardly detected within the sensitivity of our data. The best fit to the data is obtained for a column density of benzene of 5×10^{15} cm^{-2} and a kinetic temperature of 200 K. The other infrared-active bands of benzene, ν_{12}, ν_{13}, and ν_{14} (3047.908, 1483.9854, and 1038.267 cm^{-1}, respectively), have vibrational band strengths of 80.6, 31.2, and 18.2 cm^{-2} atm^{-1}, respectively, at 296 K (Dang-Nhu & Plíva 1989). Only the ν_{12} band could show significant absorption ($\simeq$1%) in the *ISO*/SWS data.

Benzene, the basic aromatic unit, has never been found outside the solar system. Large polycyclic aromatic hydrocarbons (PAHs) have been proposed as the carriers of the UIBs, but identification of specific PAH molecules has been elusive. The detection of benzene and of small species like C_4H_2, C_6H_2 indicate that the conditions in CRL 618 are right to activate a rich and diverse chemistry. Apparently, either the strong shocks associated with the 200 km s^{-1} jets or the UV photons from the rapidly evolving central object drive the polymerization of acetylene and the formation of benzene. Previously, the chemical kinetic formation of large aromatic species has been modeled for the outflows of AGB stars based on the similarity with soot formation processes in terrestrial combustion environments (Frenklach & Feigelson 1989; Cherchneff, Barker, & Tielens 1992). However, we see no evidence for di- or triacetylene or benzene in the archetype AGB object IRC +10216.

This suggests that PAH formation is linked to the chemical processing during the post-AGB phase and may actually proceed through different chemical routes than previously thought. In particular, because of the fuel-rich conditions of CRL 618 ($C/O > 1$), polymerization of acetylene may be prominently involved (Frenklach et al. 1984). In any case, our results suggest that the observed rapid evolution in the IR spectral characteristics during the transition from the AGB phase to the planetary nebula phase (Buss et al. 1990, 1993) reflects an active chemistry culminating in the formation of the UIB carriers. In the accompanying Letter (Cernicharo et al. 2001), we present the detection at millimeter wavelengths of CH_3CCH and CH_3C_4H in CRL 618 and the evidence for these and other small hydrocarbons in the *ISO* spectrum of this source.

J. C., F. H., and J. R. P. acknowledge Spanish DGES for this research under grants PB96-0883 and ESP98-1351E. J. C. and J. R. P. thank the NSF for support under grants AST 99-80846 and ATM 96-16766. IA3 is a joint development of the SWS consortium. Contributing institutes are SRON, MPE, KUL, and the ESA Astrophysics Division. We thank our anonymous referee for useful comments on the manuscript.

REFERENCES

Airé, E., & Johns, J. W. C. 1992, J. Mol. Spectrosc., 155, 195
Bujarrabal, V., Gómez-González, J., Bachiller, R., & Martín-Pintado, J. 1988, A&A, 204, 242
Buss, R. H., Jr., Cohen, M., Tielens, A. G. G. M., Werner, M. W., Bregman, J. D., Witteborn, F. C., Rank, D., & Sandford, S. A. 1990, ApJ, 365, L23
Buss, R. H., Jr., Tielens, A. G. G. M., Cohen, M., Werner, M. W., Bregman, J. D., & Witteborn, F. C. 1993, ApJ, 415, 250
Cernicharo, J., Guélin, M., & Kahane, C. 2000, A&AS, 142, 181
Cernicharo, J., Guélin, M., Peñalver, J., Martín-Pintado, J., & Mauersberger, R. 1989, A&A, 222, L1
Cernicharo, J., Heras, A. M., Pardo, J. R., Tielens, A. G. G. M., Guélin, M., Dartios, E., Neri, R., & Waters, L. B. F. M. 2001, ApJ, 546, L127
Cernicharo, J., Yamamura, I., González-Alfonso, E., de Jong, T., Heras, A., Escribano, R., & Ortigoso, J. 1999, ApJ, 526, L41
Cherchneff, I., Barker, J. R., & Tielens, A. G. G. M. 1992, ApJ, 401, 269
de Graauw, Th., et al. 1996, A&A, 315, L49
Deguchi, S., & Uyemura, M. 1984, ApJ, 285, 153
Dnag-Nhu, M., Blanquet, G., & Raulin, F. 1988, J. Mol. Spectrosc., 134, 237
Dnag-Nhu, M., & Plíva, J. 1989, J. Mol. Spectrosc., 138, 423
Fouks, B. I., & Schubert, J. 1995, Proc. SPIE, 2475, 487
Frenklach, M., Clary, D. W., Gardiner, W. C., & Stein, S. E. 1984, in 20th Symp. (Int.) on Combustion (Pittsburgh: The Institute), 887
Frenklach, M., & Feigelson, E. D. 1989, ApJ, 341, 372
Haas, S., Yamada, K. M. T., & Winnewisser, G. 1994a, J. Mol. Spectrosc., 164, 445
Haas, S., et al. 1994b, J. Mol. Spectrosc., 167, 176
Haas, S., et al. 1994c, Canadian J. Phys., 72, 1165
Herpin, F., & Cernicharo, J. 2000, ApJ, 530, L129
Herzberg, G. 1964, Molecular Spectra and Molecular Structure, Vol. 2 (Princeton: Van Nostrand)
Kahane, C., Cernicharo, J., Gómez-González, J., & Guélin, M. 1992, A&A, 256, 235
Kauppinen, J., Jensen, P., & Brodersen, S. 1980, J. Mol. Spectrosc., 83, 161
Kester, D., et al. 2000, Proc. *ISO* beyond the Peaks: The Second *ISO* Workshop on Analytical Spectroscopy (ESA SP-456; Noordwijk: ESA), in press
Khilifi, M., et al. 1995, J. Mol. Spectrosc., 174, 116
Kwok, S., & Feldman, P. A. 1981, ApJ, 247, L67
Lahuis, F., et al. 1998, ASP Conf. Ser. 145, Astronomical Data Analysis Software and Systems VII, ed. R. Albrecht, R. N. Hook, & H. A. Bushouse (San Francisco: ASP), 224
Lindemayer, J., Magg, U., & Jones, H. 1988, J. Mol. Spectrosc., 128, 172
Martín-Pintado, J., Gaume, R., Bachiller, R., & Johnston, K. 1993, ApJ, 419, 725
McNaughton, D., & Bruget, D. N. 1991, J. Mol. Spectrosc., 150, 620
———. 1992, J. Mol. Struct., 273, 11
Salama, A., et al. 1997, in The First *ISO* Workshop on Analytical Spectroscopy, ed. A. M. Heras, K. Leech, N. R. Trams, & M. Perry (ESA SP-419; Noordwijk: ESA), 17
Uyemura, M., Deguchi, S., Nakada, Y., & Onaka, T. 1982, Bull. Chem. Soc. Japan, 55, 384
Yamada, K. M. T., & Bürger, H. 1986, Z. Naturforsch, 41a, 1021